大阪公立大学
Osaka Metropolitan University
学術情報リポジトリ

Unbalanced Voltage Control of Three-phase Induction Motor by Thyristors

メタデータ	言語: eng
	出版者:
	公開日: 2010-04-05
	キーワード (Ja):
	キーワード (En):
	作成者: Fujii, Tomoo, Sako, Kuniaki, Ishizaki, Takemitsu
	メールアドレス:
	所属:
URL	https://doi.org/10.24729/00008752

Unbalanced Voltage Control of Three-phase Induction Motor by Thyristors

Tomoo FUJII*, Kuniaki SAKO** and Takemitsu ISHIZAKI*

(Received November, 15, 1973)

This paper deals with an analytic means of the characteristics of a three-phase induction motor whose primary voltage is controlled by an inverse parallel connected pair of thyristors in series with one of the stator windings. On this control, waveforms of the primary phase voltage of the motor are different from each other. As a result of the unbalance of primary voltage the currents flowing in the stator windings become unbalanced.

Therefore, analysis of the characteristics of the motor is carried out through the Fourier analysis of the primary voltage and the symmetorical co-ordinates method. This method follows fairly simpler results than ones given in the other papers. The analytical results agree well with experimental ones and are accurate enough for practical usage.

1. Introduction

Unbalanced primary voltage control of a three-phase induction motor by thyristors is one of the speed control methods which is taken by varying the positive-phase-sequence component of primary voltage. By delaying the firing angle of thyristors connected in series with one or two of the stator windings, the currents on each phase become unbalanced and the positive-phase-sequence component of the motor supply voltage is equivalently decreased.

It is legitimate to analyze the transient or steady-state characteristics of the motor on this control by using differential equations on each period, which is set up from the motor operational conditions and the firing angle of thyristors, and by connecting the boundary conditions of these equations.[1,2,3,4] But this method is rather complicated one for the purpose of deriving only the steady-state characteristics.

Therefore, this paper deals with the relatively simple method to obtain the approximate steady-state characteristics of the motor whose primary voltage is controlled by an inverse parallel pair of thyristor in series with one of the stator windings. In this method, the Fourier analysis and the symmetorical co-ordinate method are applied, and the motor characteristics are obtained by assuming that the motor is driven under unbalanced sinusoidal voltage source.

Waveforms of the primary voltage, to which the Fourier analysis is applied, are decided by the firing angle and the conduction angle of thyristors inserted in the main circuit. The firing angle can be chosen arbitrarily from the control circuit, but

* Department of Electrical Engineering, College of Engineering.
** Graduate Student, Department of Electrical Engineering, College of Engineering.

the conduction angle depends on the firing angle, the equivalent circuit constants, speed and counter e. m. f. which appears in the primary voltage during the cut-off period of the thyristor pair.

The results obtained by this analysis agree well with experimental ones and are applicable for practical usage.

2. Analysis

The main circuit of a three-phase induction motor whose primary voltage is controlled by a thyristor pair is shown in Fig. 1.

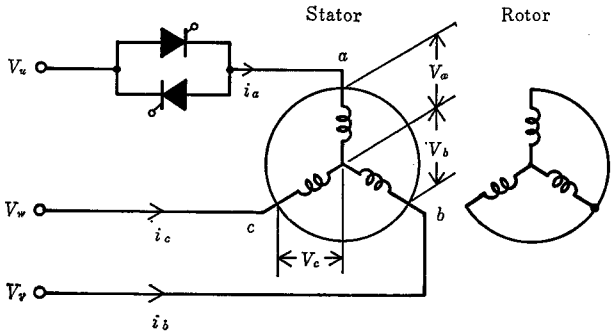

Fig. 1. Main circuit of unbalanced voltage control of three phase induction motor.

The characteristics of the induction motor excited by the unbalanced three-phase voltage are obtained through the symmetorical co-ordinates method, where the zero-phase-sequence component of the voltage does not influence the motor characteristics, because the neutral of the stator windings is not connected to the source.

2.1 Primary Voltage Waveforms

Typical waveforms of the line-to-neutral voltage of the motor are shown in Figs. 2 and 3. Fig. 2 is of theoretical waveforms, and Fig. 3 is of oscillograms corresponding to Fig. 2. In these figures the slip s is 4 percent and the firing angle is 90 degrees.

As shown in these figures the primary voltage waveforms differ with each winding. The distortion of waveforms is caused by the displacement of the electrical neutral point of stator windings during the interval when the thyristor pair is cut-off. The displacement of the neutral is influenced by the counter e. m. f. induced by the rotor current. However, it is not easy to determine the counter e. m. f. quantitatively when the motor has any cut-off operation periods during one half cycle of the source voltage as on this control.

In the case that a three-phase induction motor is excited by balanced sinusoidal voltage, the counter e. m. f. is also balanced, and will be expressed as the terminal voltage of the equivalent resister $\frac{1-s}{s}r_2'$ in the equivalent circuit per phase of the motor. Assuming that the counter e. m. f. on the balanced control is applicable on

$\alpha=90°$, S$=4\%$, $\beta=102.2°$, $\phi_g=8.35$, A$=0.904$ 904

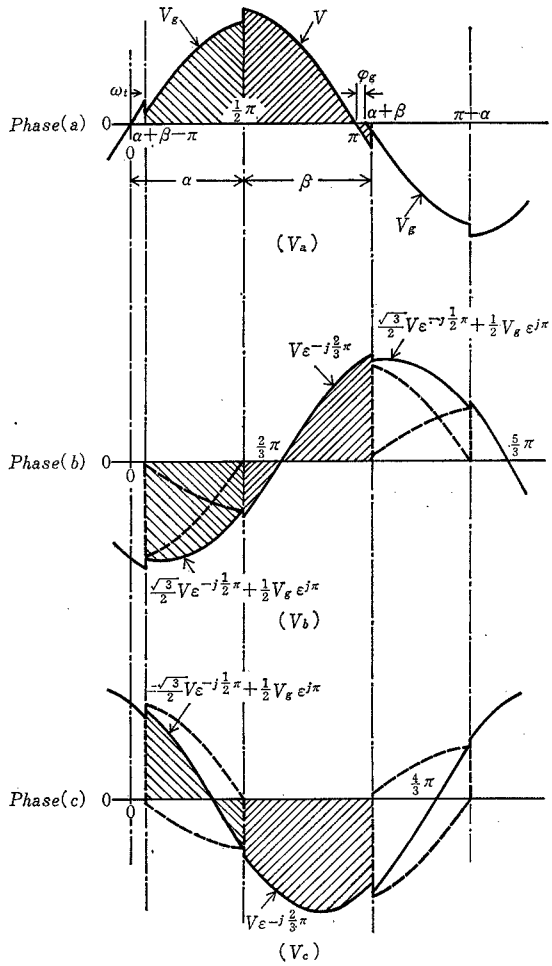

Fig. 2. Stator voltage wave forms on each phase.

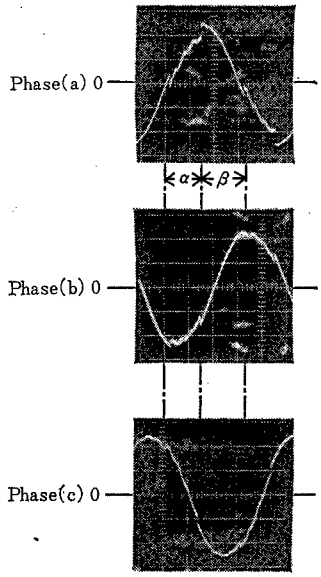

Fig. 3. Ocsillograms of stator voltage waveform.

this unbalanced control, the counter e. m. f. $\dot{V}_g$ is expressed as Eq. (1).

$$\dot{V}_g=\dot{V}\frac{(1-s)r_2'}{(r_2'+jsx_2')+s(r_1+jx_1)+(r_1+jx_1)(r_2'+jx_2')\dot{Y}_0} \tag{1}$$

where

$\dot{V}$: line-to-neutral voltage of the source

r_1, x_1: stator resistance and leakage reactance per phase

r_2', x_2': rotor resistance and leakage reactance per phase refered to stator

$\dot{Y}_0$: magnetizing admittance per phase, $(=g_0-jb_0)$

s: motor speed in slip.

Defining $\dot{V}_g$ as above, the neutral position of stator windings is determined on the vector diagram with the slip s as a variable. Then the vector diagram of primary

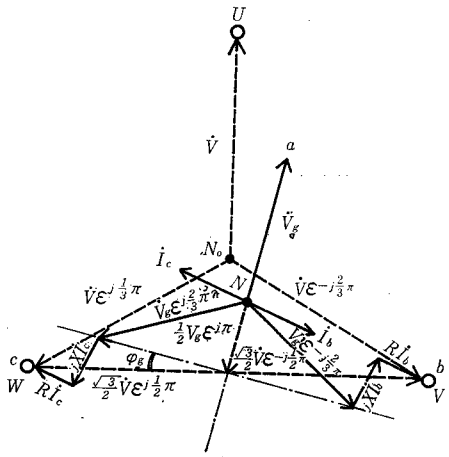

Fig. 4. Vector diagram of stator volage.

voltage during the cut-off interval of a thyristor pair is described as Fig. 4.

And the three-phase input terminal-to-neural voltages of the motor $\dot{V}_a$, $\dot{V}_b$ and $\dot{V}_c$ are formulized as follows,

$$\left.\begin{aligned}\dot{V}_a&=\dot{V}_g\\ \dot{V}_b&=\frac{\sqrt{3}}{2}\dot{V}\varepsilon^{-j\frac{1}{2}\pi}+\frac{1}{2}\dot{V}_g\varepsilon^{j\pi}\\ \dot{V}_c&=\frac{\sqrt{3}}{2}\dot{V}\varepsilon^{j\frac{1}{2}\pi}+\frac{1}{2}\dot{V}_g\varepsilon^{j\pi}\end{aligned}\right\}\qquad(2)$$

where

$\dot{V}$: line-to-neutral voltage of phase U

$\dot{V}_g$: counter e. m. f. for the stator winding a.

During the on interval of the thyristor pair, $\dot{V}_a$, $\dot{V}_b$ and $\dot{V}_c$ are indentical with line-to-neutral voltages $\dot{V}_U$, $\dot{V}_V$ and $\dot{V}_W$ respectively.

2.2 Analysis of Primary Voltage Waveforms

As shown in Figs. 2 and 3, the distorted waveforms of primary voltage for small slip s are similar to sinwaves. Therefore, in order to obtain the approximate characteristics of the motor it is sufficient that the Fourier analysis for the primary voltage is carried out only for the line frequency component.

Now terming the line frequency components of primary voltages v_{a1}, v_{b1} and v_{c1} corresponding with v_a, v_b and v_c respectively, they are expressed as follows,

$$v_{a1}=\frac{1}{2\pi}V\sqrt{A_{a1}^2+B_{a1}^2}\sin(\omega t+\theta_{a1})\qquad(3)$$

where

$$A_{a1}=2[\beta-\cos(2\alpha+\beta)\sin\beta+K\{\cos(2\alpha+\beta-\varphi_g)\sin\beta+(\pi-\beta)\cos\varphi_g\}]$$
$$B_{a1}=2[\sin(2\alpha+\beta)\sin\beta-K\{\sin(2\alpha+\beta-\varphi_g)\sin\beta-(\pi-\beta)\sin\varphi_g\}]$$
$$\theta_{a1}=\tan^{-1}\frac{B_{a1}}{A_{a1}}$$

α: firing angle of thyristors

β: conduction angle of thyristors

V: peak value of line-to-neutral voltage

K: ratio of peak value of V_g to V

$$K=\left|\frac{(1-s)r_2'}{(r_2'+jsx_2')+s(r_1+jx_1)+(r_1+jx_1)(r_2'+jx_2')\dot{Y}_0}\right| \tag{4}$$

φ_g: phase difference of V and V_g

$$\varphi_g=\tan^{-1}\left\{\frac{s(x_2'+x_1)+g_0(sr_1x_2'+x_1r_2')-b_0(r_1r_2'-sx_1x_2')}{(r_2'+sr_1)+g_0(r_1r_2'-sx_1x_2')+b_0(sr_1x_2'+x_1r_2')}\right\} \tag{5}$$

$$v_{b1}=\frac{1}{2\pi}V\sqrt{A_{b1}^2+B_{b1}^2}\sin\left(\omega t+\theta_{b1}-\frac{2}{3}\pi\right) \tag{6}$$

where

$$A_{b1}=\frac{1}{2}(3\pi+\beta)+\cos\left(2\alpha+\beta-\frac{2}{3}\pi\right)$$
$$+K\left\{(\pi-\beta)\cos\left(\frac{1}{3}\pi+\varphi_g\right)-\cos\left(2\alpha+\beta-\frac{2}{3}\pi-\varphi_g\right)\sin\beta\right\}$$

$$B_{b1}=\frac{\sqrt{3}}{2}(\pi-\beta)-\sin\left(2\alpha+\beta-\frac{2}{3}\pi\right)$$
$$-K\left\{(\pi-\beta)\sin\left(\frac{1}{3}\pi+\varphi_g\right)-\sin\left(2\alpha+\beta-\frac{2}{3}\pi-\varphi_g\right)\sin\beta\right\}$$

$$\theta_{b1}=\tan^{-1}\frac{B_{b1}}{A_{b1}}$$

and

$$v_{c1}=\frac{1}{2\pi}V\sqrt{A_{c1}^2+B_{c1}^2}\sin\left(\omega t+\theta_{c1}+\frac{2}{3}\pi\right) \tag{7}$$

where

$$A_{c1}=\frac{1}{2}(3\pi+\beta)+\cos\left(2\alpha+\beta+\frac{2}{3}\pi\right)\sin\beta$$
$$+K\left\{(\pi-\beta)\cos\left(\frac{1}{3}\pi-\varphi_g\right)-\cos\left(2\alpha+\beta+\frac{2}{3}\pi-\varphi_g\right)\sin\beta\right\}$$

$$B_{c1}=\frac{\sqrt{3}}{2}(\pi-\beta)-\sin\left(2\alpha+\beta+\frac{2}{3}\pi\right)\sin\beta$$
$$-K\left\{(\pi-\beta)\sin\left(\frac{1}{3}\pi-\varphi_g\right)+\sin\left(2\alpha+\beta+\frac{2}{3}\pi-\varphi_g\right)\sin\beta\right\}$$

$$\theta_{c1}=\tan^{-1}\frac{B_{c1}}{A_{c1}}.$$

During the cut-off interval of the thyristor pair, a-phase current does not flow, but the counter e. m. f. appears in a-phase stator winding. Therefore, the a-phase voltage during the period $\alpha+\beta-\pi\leqq\omega t\leqq\alpha$ in Fig. 2 should be excepted from the analysis. Then A_{a1} and B_{a1} are reduced as follows,

$$A_{a1}=2\{\beta-\cos(2\alpha+\beta)\sin\beta\}$$
$$B_{a1}=2\sin(2\alpha+\beta)\sin\beta$$

2.3 Calculation of conduction angle

The analytical method of state variable is legitimate on the calculation of conduc-

tion angle of thyristor in Fig. 1, but it is so complicated and not applicative in practice. Then in this article how to calculate the conduction angle according to the circuit shown in Fig. 5 is described.

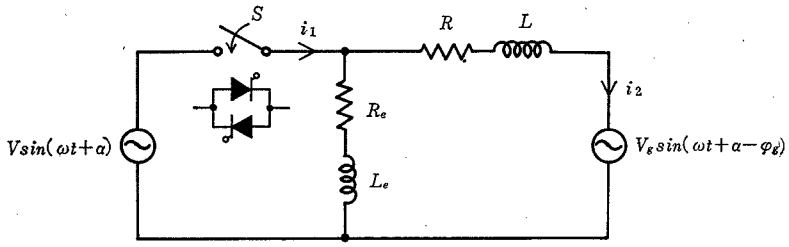

$R=r_1+r'_2,\ L=\frac{1}{\omega}(x_1+x'_2),\ R_e=\frac{g_o}{\sqrt{g_o^2+b_o^2}},\ L=\frac{b_o}{\omega\sqrt{g_o^2+b_o^2}}$

Fig. 5. Circuit for calculation of conduction angle of thyristor.

The circuit is based on the equevalent circuit of a three-phase induction motor for the positive-phase-sequence component of exciting voltage with regard to the counter e. m. f. of the motor. In order to make the calculation more simple, the L-type equivalent circuit of the three-phase induction motor is adopted. The conduction angle of thyristor is calculated as follows,

<First Period> $0\leqq\omega t\leqq\beta$, from the time when the thyristor of positive direction turns on until the time when it turns off.

The fundamental diffential equations of the circuit in Fig. 5 are expressed,

$$\left.\begin{aligned} &L\frac{di_{2,1}}{dt}+Ri_{2,1}+V_g\sin(\omega t+\alpha-\varphi_g)=V\sin(\omega t+\alpha)\\ &L_e\frac{d}{dt}(i_{1,1}-i_{2,1})+R_e(i_{1,1}-i_{2,1})=V\sin(\omega t+\alpha)\end{aligned}\right\}\qquad(8)$$

where $i_{1,1}$ and $i_{2,1}$ are the currents i_1 and i_2 in Fig. 5 respectively during this period. From these equations the currents $i_{1,1}$ and $i_{2,1}$ result in

$$\left.\begin{aligned} i_{1,1}(t)=&V\Big[\frac{1}{\sqrt{R_e^2+\omega^2L_e^2}}\Big\{\sin(\omega t+\alpha-\varphi_e)-\sin(\alpha-\varphi_e)\varepsilon^{-\frac{R_e}{L_e}t}\Big\}\\ &+\frac{1}{\sqrt{R^2+\omega^2L^2}}\Big\{\sin(\omega t+\alpha-\varphi)-\sin(\alpha-\varphi)\varepsilon^{-\frac{R}{L}t}\Big\}\Big]\\ &+V_g\frac{1}{\sqrt{R^2+\omega^2L^2}}\Big\{\sin(\omega t+\alpha-\varphi_g-\varphi)-\sin(\alpha-\varphi_g-\varphi)\varepsilon^{-\frac{R}{L}t}\Big\}\\ &+i_{2,1}(0)\Big(\varepsilon^{-\frac{R}{L}t}-\varepsilon^{-\frac{R_e}{L_e}t}\Big)\\ i_{2,1}(t)=&V\frac{1}{\sqrt{R^2+\omega^2L^2}}\Big\{\sin(\omega t+\alpha-\varphi)-\sin(\alpha-\varphi)\varepsilon^{-\frac{R}{L}t}\Big\}\\ &+V_g\frac{1}{\sqrt{R^2+\omega^2L^2}}\Big\{\sin(\omega t+\alpha-\varphi_g-\varphi)-\sin(\alpha-\varphi_g-\varphi)\varepsilon^{-\frac{R}{L}t}\Big\}\\ &+i_{2,1}(0)\varepsilon^{-\frac{R}{L}t}\end{aligned}\right\}\qquad(9)$$

where

$$\varphi=\tan^{-1}\frac{\omega L}{R}$$

$$\varphi_e=\tan^{-1}\frac{\omega L_e}{R_e}.$$

<Second Period> $\beta\leqq\omega t\leqq\pi$, from the time when the thyristor of positive direction turns off until the time when the thyristor of negative direction turns on.

The current i_1 does not flow during this period. Therefore the differential equation of the circuit in Fig. 5 is expressed as follows,

$$(L+L_e)\frac{di_{2,2}}{dt}+(R+R_e)i_{2,2}+V_q\sin(\omega t+\alpha-\varphi_q)=0 \tag{10}$$

where $i_{2,2}$ is the current i_2 during this period.

Then $i_{2,2}$ results in

$$i_{2,2}(t)=-\frac{V_q}{\sqrt{(R+R_e)^2+\omega^2(L+L_e)^2}}\Big\{\sin(\omega t+\alpha-\varphi_q-\varphi')$$
$$-\sin(\alpha+\beta-\varphi_q-\varphi')\varepsilon^{-\frac{R+R_e}{L+L_e}\left(t-\frac{\beta}{\omega}\right)}\Big\}+i_{2,2}\left(\frac{\beta}{\omega}\right)\varepsilon^{-\frac{R+R_e}{L+L_e}\left(t-\frac{\beta}{\omega}\right)} \tag{11}$$

where

$$\varphi'=\tan^{-1}\frac{\omega(L+L_e)}{R+R_e}$$

Rearranging Eqs. (9) and (11) by substituting the boundary conditions of currents expressed as Eqs. (12) and (13) into,

$$\left.\begin{aligned} i_{1,1}\left(\frac{\beta}{\omega}\right)&=0\\ i_{2,1}\left(\frac{\beta}{\omega}\right)&=i_{2,2}\left(\frac{\beta}{\omega}\right)\end{aligned}\right\} \tag{12}$$

and in steady state,

$$i_{2,2}\left(\frac{\beta}{\omega}\right)=-i_{2,1}(0), \tag{13}$$

ultimately the relation among the firing angle α, the conduction angle β and slip s is given in Eq. (14).

$$\frac{\varepsilon^{-\frac{R}{\omega L}\beta}-\varepsilon^{-\frac{R_e}{\omega L_e}\beta}}{1+\varepsilon^{-\frac{R}{\omega L}\beta}\cdot\varepsilon^{\frac{R+R_e}{\omega(L+L_e)}(\beta-\pi)}}\left\{F_1+F_2\varepsilon^{\frac{R+R_e}{\omega(L+L_e)}(\beta-\pi)}\right\}=F_2+F_3 \tag{14}$$

where

$$F_1=\frac{K}{\sqrt{(R+R_e)^2+\omega^2(L+L_e)^2}}\left\{\sin(\alpha+\beta-\varphi_q-\varphi')\varepsilon^{-\frac{R+R_e}{\omega(L+L_e)}\beta}+\sin(\alpha-\varphi_q-\varphi')\right\}$$

$$F_2=\frac{1}{\sqrt{R^2+\omega^2L^2}}\Big[\sin(\alpha+\beta-\varphi)-\sin(\alpha-\varphi)\varepsilon^{-\frac{R}{\omega L}\beta}$$
$$-K\left\{\sin(\alpha+\beta-\varphi-\varphi_q)-\sin(\alpha-\varphi_q-\varphi)\varepsilon^{-\frac{R}{\omega L}\beta}\right\}\Big]$$

$$F_3=\frac{1}{\sqrt{R_e^2+\omega^2L_e^2}}\left\{\sin(\alpha+\beta-\varphi_e)-\sin(\alpha-\varphi_e)\varepsilon^{-\frac{R_e}{\omega L_e}\beta}\right\}.$$

The calculated results of Eq. (14) and the measured values of conduction angle are shown in Fig. 6.

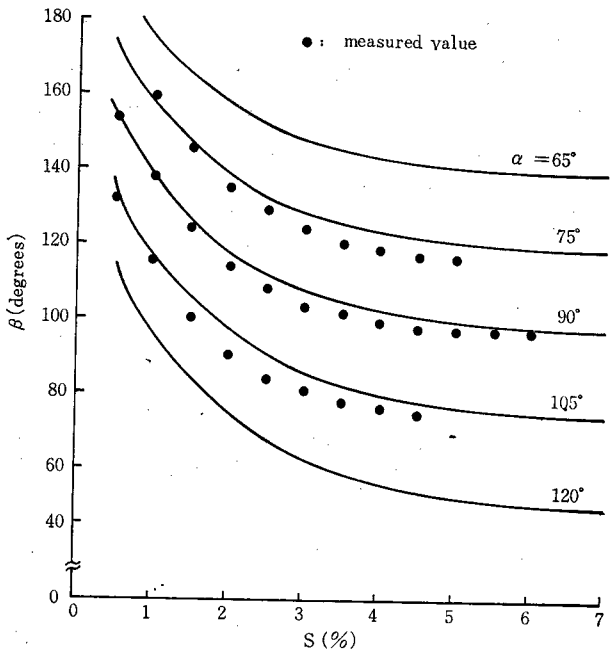

Fig. 6. Rerations of slip s $v.s$ conduction angle β.

3. Theoretical and Experimental Results

The theoretical characteristics of the three-phase induction motor on this unbalanced voltage control can be calculated by applying the symmetorical co-ordinates method and the equevalent circuit of the motor to the line frequency components v_{a1}, v_{b1} and v_{c1} obtained previously.

The theoretical and experimental results of primary current and torque are shown in Fig. 7, where the source line-to-neutral voltage is $50\sqrt{3}$ volts and the firing angle α is 75 degrees.

The ratings of the tested three-phase wound-rotor induction motor are as follows,

output : 2.2(KW), voltage : 220(V), current : 8.2(A), frequency : 60(Hz),

and the equevalent circuit constants are as follows,

$$r_1=0.986\ (\Omega),\quad r_2'=0.784\ (\Omega),\quad x_1=x_2'=1.51\ (\Omega)$$

$$g_0=0.002\ (\mho),\quad b_0=0.024(\mho).$$

The difference between the experimental results and the theoretical ones noticed in Fig. 7 is considered to be due to an error which is caused by assuming that the counter e. m. f. of the motor on this control is expressed as Eq. (1). Therefore, this difference might be decreased if the counter e. m. f. is determined with higher accuracy.

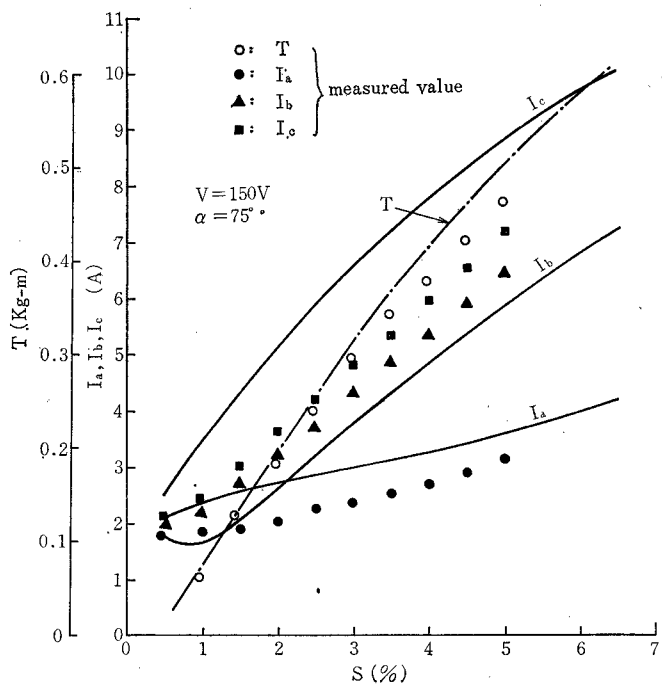

Fig. 7. Characteristics of slip *s v.s* torque T and currents.

4. Conclution

Analytical means of the characteristics of the three-phase induction motor whose primary voltage is controlled by thyristors tends to become hard to apply in practice. Then in order to simplify the analysis, the approximate characteristics of the motor on this control are obtained by using the equivalent circuit of the motor, which is well known, on this analysis. The results calculated by this means are accurate enough for practical application.

The problem that have been left unsettled in this analysis is to determine the counter e. m. f. of the motor more accurately. This is the common problem on the motor control when the primary voltage is controlled by chopping the source voltage, and will be discussed elsewhere.

References

1) T. A. Lipo, IEEE Trans. PAS-**90** No. 2, 515 (1972)
2) T. Takeuchi, Theory of SCR Circuit and Applycation to Motor Control, OHM Co., Tokyo (1968)
3) N. Hayashi, J. I. E. E. of Japan **91**-12, 171 (1971)
4) N. Hayashi, J. I. E. E. of Japan, **92B**-1, 29 (1972)